# Enhanced Hydrocracking Performance of NiW/Zeolite Beta-γ-$Al_2O_3$ Catalyst: Effect of Hydrothermal Crystallization on Acidity and Catalytic Activity

Lailatul Badriyah [1,2*], Istadi[1], Wawan Rustyawan[2], Syifa Urrohmah[3], Yulyani Nur Azizah[3]

[1]*Department of Chemical Engineering, Faculty of Engineering, Diponegoro University, Tembalang, Semarang, 50239, Indonesia*
[2]*Technology Innovation & Implementation, P.T. Pertamina, Jakarta, Indonesia*
[3]*Department of Chemistry, Faculty of Science and Technology, Syarif Hidayatullah State Islamic University Jakarta, South Tangerang, 15412, Indonesia*

**Corresponding Author. E-mail: lailatulbadriyah@students.undip.ac.id / lbadriyah732@gmail.com (Lailatul Badriyah)*

Accepted Manuscript - BCREC-20881 - 26 Nov 2026

**Abstract**

The development of efficient hydrocracking catalysts is crucial to meet the increasing demand for light fuel fractions, particularly from alternative feedstocks such as Hydrotreated Vegetable Oil (HVO). Although NiW-based and zeolite-supported catalysts have been widely studied, the influence of zeolite beta synthesis conditions on acidity properties and their implications for catalytic performance remains insufficiently understood. This study aims to evaluate the effect of zeolite beta crystallization temperature on the physicochemical characteristics and catalytic activity of NiW/Zeolite beta-γ-$Al_2O_3$ catalysts in hydrocracking processes. Zeolite beta was synthesized via a hydrothermal method at crystallization temperatures of 135 and 170°C, followed by combination with γ-$Al_2O_3$ as a support and impregnation with Ni and W as active metals to produce a bifunctional catalyst. Catalyst characterization was conducted using X-Ray Diffraction (XRD), X-Ray Fluorescence (XRF), Surface Area Analyzer (SAA), and Temperature Programmed Desorption of $NH_3$ ($NH_3$-TPD) to examine crystal structure, elemental composition, surface area and total acidity. The result indicates that higher crystallization temperatures lead to catalysts with increased surface area and total acidity, which are associated with higher hydrocracking activity. Performance testing of the optimal (crystalline) catalyst in a fixed-bed reactor showed that the NiW/Zeolite beta-γ-$Al_2O_3$ catalyst achieved a maximum conversion of 66.81% at 360°C, which was higher than that of the reference catalyst (22.40%). This study provides evidence that links the crystallization temperature of zeolite beta to the total acidity and the hydrocracking performance of NiW-based catalysts for HVO conversion. These findings suggest that optimizing zeolite synthesis parameters is a promising strategy for designing NiW-based hydrocracking catalysts.

**Keywords:** Hydrocracking, NiW Catalyst, Beta Zeolite, Hydrothermal Synthesis, Total Acidity, HVO

## 1. Introduction

The increasing demand for light fuel fractions has driven the development of technologies for converting heavy hydrocarbons into high-value products, such as naphtha, kerosene, and diesel. One of

the most widely employed technologies is hydrocracking, a catalytic process that converts long-chain hydrocarbons into lighter molecules through the simultaneous occurrence of cracking and hydrogenation reactions over bifunctional catalysts. Compared with thermal cracking, hydrocracking produces higher-quality fuels with lower sulfur content and higher cetane numbers [1][2].

The performance of the hydrocracking process is strongly influenced by the physicochemical properties of the catalyst. Beta zeolite is considered a promising catalyst support due to its three-dimensional pore structure, high surface area, excellent thermal stability, and suitable acidity for hydrocarbon cracking reactions [3] [4]. To improve its mechanical strength and textural properties, Beta zeolite is commonly combined with γ-$Al_2O_3$ as a binder [5]. In addition, active metal components are incorporated to provide hydrogenation functionality. Among various transition metal systems, nickel–tungsten (NiW) catalysts exhibit superior hydrogenation activity and higher sulfur tolerance compared with conventional NiMo and CoMo catalysts [6] .

Previous studies have demonstrated that Beta zeolite enhances hydrocracking activity and product selectivity by improving acid site accessibility and increasing the catalyst surface area. The incorporation of Beta zeolite into catalyst systems has also been reported to enhance acidity, specific surface area, and the conversion of middle-distillate products [2,6,7]. However, the influence of the structural characteristics of synthesized Beta zeolite supports on the catalytic performance of NiW catalysts during hydrocracking has not been comprehensively investigated.

Therefore, this study aims to synthesize Beta zeolite via the hydrothermal method, prepare NiW-supported β-zeolite/γ-$Al_2O_3$ catalysts, and evaluate their physicochemical properties and catalytic performance in the hydrocracking of Hydrotreated Vegetable Oil (HVO). Catalyst characterization was carried out using X-ray Diffraction (XRD), X-ray Fluorescence (XRF), Surface Area Analysis (BET), and Temperature-Programmed Desorption of Ammonia ($NH_3$-TPD). Catalytic performance was evaluated on the crystalline catalyst, which was selected based on the characterization results, and on the reference catalyst in a fixed-bed reactor at reaction temperatures of 330, 345, and 360 °C.

## 2. Experimental

### 2.1. Materials

Silica, deionized water, tetraethylammonium hydroxide (TEAOH, Merck 108123), sodium chloride (NaCl, Merck 106404), potassium chloride (KCl, Merck 104936), sodium hydroxide (NaOH, Merck), sodium aluminate (Sigma-Aldrich), boehmite, nitric acid ($HNO_3$, Merck 100456), ammonia solution ($NH_4OH$, Merck 105432), ammonium nitrate ($NH_4NO_3$, Merck 101188), nickel nitrate hexahydrate ($Ni(NO_3)_2{\cdot}6H_2O$, Merck), ammonium metatungstate hydrate ($(NH_4)_6H_2W_{12}O_{40}{\cdot}xH_2O$, E-Merck, Germany), Hydrotreated Vegetable Oil (HVO) supplied by PT Pertamina (Persero), and high-purity $O_2$, $H_2$, and $N_2$ gases were used as starting materials without further purification.

Accepted Manuscript - BORE-20881 - 26 Nov 2026

## 2.2. Catalyst Preparation

### 2.2.1. Synthesis of Beta Zeolite

Beta zeolite was synthesized via the hydrothermal method according to the procedure reported by Pertamina (2015). Solution A was prepared by mixing 29 g of double-distilled water, 44.8 g of TEAOH solution (10 wt.%), 0.265 g of NaCl, and 0.72 g of KCl, followed by homogenization. Silica (14.77 g) was then added and homogenized. Solution B was prepared from 10 g of double-distilled water, 0.165 g of NaOH, and 0.896 g of $NaAlO_2$. Solution B was added to Solution A and stirred for 10 min. The molar composition of the synthesis gel was 1 $SiO_2$ : 0.022 $Al_2O_3$ : 0.12 TEAOH : 0.031 $Na_2O$ : 0.018 NaCl : 0.039 KCl : 17.9 $H_2O$, corresponding to a Si/Al molar ratio of 22.5. The gel was transferred into an autoclave and crystallized at 135 and 170 °C for 22 h. The product was filtered and dried at 100 °C until completely dry.

### 2.2.2. Preparation of Beta Zeolite Support

The Beta zeolite support was prepared following the procedure reported by Pertamina (2015). Beta zeolite (25 g) and boehmite (5 g; zeolite-to-binder mass ratio of 5:1) were mixed as the catalyst support and binder, respectively, followed by the addition of 8 mL of double-distilled water and homogenization for 1 min. Then, 27 mL of 5 wt.% nitric acid was added and the mixture was homogenized for 15 min, after which 4 mL of 25 wt.% ammonium hydroxide was added and kneaded until a homogeneous, cohesive paste was obtained. The paste was extruded into a trilobe shape using a hydraulic extruder, dried at 120 °C for 1 h, and calcined at 550 °C for 5 h to obtain the Beta–γ-$Al_2O_3$ support. The support was characterized by XRD, XRF, SAA, and $NH_3$-TPD.

### 2.2.3. Preparation of NiW/Beta–γ-$Al_2O_3$ Catalyst

The NiW/Beta–γ-$Al_2O_3$ catalyst was prepared by the dry (incipient wetness) impregnation method according to the procedure reported by Pertamina (2015). An impregnation solution was prepared by dissolving 9 g of nickel nitrate hexahydrate ($Ni(NO_3)_2{\cdot}6H_2O$) in 20 mL of double-distilled water under stirring until homogeneous, followed by the addition of 12 g of ammonium metatungstate hydrate ($(NH_4)_6H_2W_{12}O_{40}{\cdot}xH_2O$) and stirring until completely dissolved. The solution was then impregnated onto 28.5 g of the Beta–γ-$Al_2O_3$ support by placing the support and the solution in a container and shaking until completely mixed, with target loadings of 2 wt.% NiO and 15 wt.% $WO_3$. The impregnated catalyst was dried at 120 °C for 2 h and calcined at 450 °C for 3 h, and then characterized by XRD, XRF, SAA, and $NH_3$-TPD prior to catalytic performance evaluation.

### 2.2.4. Reference Catalyst

The reference catalyst was commercial composition (NiO 1.80 and 13.00 $WO_3$ wt.%). Its metal content, textural properties, and acidity are given in Tables 1–3.

Accepted Manuscript - BCREC 20881 - 26 Nov 2025

2.3. Catalyst Characterization

The synthesized catalysts were characterized to evaluate their crystal structure, elemental composition, textural properties, and surface acidity. The crystalline phases were identified by X-ray diffraction (XRD) using Cu Kα radiation operated at 40 kV and 35 mA over a 2θ range of 5–90°. The elemental composition of Ni and W was determined using X-ray fluorescence (XRF). The specific surface area, pore volume, and pore diameter were measured using a Surface Area Analyzer (SAA) based on the Brunauer–Emmett–Teller (BET) method after vacuum degassing. The surface acidity was determined by temperature-programmed desorption of ammonia ($NH_3$-TPD) to quantify the total acidity (the total amount of acid sites) from the programmed $NH_3$ desorption profile. For $NH_3$-TPD, the samples were first pretreated by heating to 120°C at 10°C $min^{-1}$ (through an intermediate 60°C step) and holding for 30 min, and then cooled to 30°C and stabilized for 20 min. The gas was subsequently switched to ammonia for 10 min for $NH_3$ adsorption at 30°C, followed by switching to helium for 30 min to remove physisorbed $NH_3$. The samples were then heated from 30 to 830°C at 20°C $min^{-1}$. The total acidity was calculated by integrating the $NH_3$ desorption profile.

2.4. Catalytic Performance Evaluation

The catalytic performance was evaluated using a PID Effi Microactivity Reactor through three sequential stages: catalyst loading, catalyst activation, and hydrocracking reaction. Approximately 10 mL of catalyst was loaded into the reactor, followed by a leak test to ensure system integrity. Catalyst activation was carried out by sulfiding with a mixture of hydrogen gas and dimethyl disulfide (DMDS) dissolved in naphtha (DMDS content of 3000 ppm at 315 °C and 30 bar for 8 h, with an $H_2$/HC ratio of 250 $Nm^3/m^{-3}$) to generate $H_2S$, which converted the active metal species from the oxide phase to the corresponding sulfide phase. The sulfided phase was not characterized, and sulfur retention during HVO conversion was not monitored in this study. After sulfiding, Hydrotreated Vegetable Oil was introduced into the reactor under operating conditions of 30 bar pressure, a liquid hourly space velocity (LHSV) of 2.5 $h^{-1}$, and an $H_2$/HC ratio of 300 $Nm^3/m^{-3}$. Hydrocracking reactions were conducted at 330, 345, and 360 °C. At each temperature, the liquid and gaseous products were collected time on stream. The resulting liquid products were analyzed using Gas Chromatography Simulated Distillation (GC-SIMDIS), while gaseous products were analyzed using Gas Chromatography (GC).

2.5. Liquid Product Analysis by GC-SIMDIS

The liquid products were characterized using Gas Chromatography Simulated Distillation (GC-SIMDIS) according to ASTM D2887. Samples were injected at an initial temperature of 100 °C and heated to 400 °C at a heating rate of 4 °C $min^{-1}$. Nitrogen and helium were employed as carrier gases at flow rates of 45 mL $min^{-1}$ and 14 mL $min^{-1}$, respectively. The GC-SIMDIS analysis was used to determine the

Accepted Manuscript - BCREC-20881 - 20 Nov 2026

hydrocarbon distribution within the $C_5$–$C_{44}$ range based on the correlation between boiling point and retention time, yielding chromatograms and carbon distribution data expressed as area percentages.

2.6. Gaseous Product Analysis by Gas Chromatography

The gaseous products were analyzed using Gas Chromatography (GC) according to ASTM D1945. Gas samples were collected in gas sampling bags and subsequently introduced into the GC system for the determination of gas composition and concentration. Analyses were performed for products obtained at reaction temperatures of 330, 345, and 360 °C.

2.7. Calculation of Conversion, Selectivity, and Yield

Conversion, selectivity, and yield were calculated from the GC-SIMDIS data using Equations (1)–(3):

$$X\ (\%) = (A_{feed} - A_{prod}) / A_{feed} \times 100 \qquad (1)$$

$$S_i\ (\%) = A_i / \Sigma A_j \times 100 \qquad (2)$$

$$Y_i\ (\%) = X \times S_i / 100 \qquad (3)$$

where X is the conversion, $S_i$ the selectivity to product fraction i, and $Y_i$ the yield of fraction i. $A_{feed}$ and $A_{prod}$ are the SIMDIS area percentages of the fraction boiling above ($C_6$-$C_{10}$ 180°C and $C_{11}$-$C_{14}$ 250°C) in the HVO feed and in the liquid product, respectively; $A_i$ is the area percentage of fraction i (naphtha, $C_6$–$C_{10}$; kerosene, $C_{11}$–$C_{14}$) in the liquid product; and $\Sigma A_j$ is the sum of the area percentages of all fractions below the cut-off. Gaseous products were analyzed only for their relative composition; because the gas flow rate was not recorded, gaseous yields and carbon balances were not calculated.

**3. Results and Discussion**

3.1. Synthesis of Beta Zeolite

The synthesis of Beta zeolite was initiated by dissolving NaCl, KCl, and tetraethylammonium hydroxide (TEAOH), followed by the addition of silica. TEAOH was employed as a structure-directing agent (SDA) to facilitate the formation of the Beta zeolite framework. [4] reported that TEAOH plays a crucial role in directing the crystallization pathway toward the formation of the Beta zeolite structure. Subsequently, sodium aluminate and NaOH were dissolved in deionized water to form a clear solution, which was then gradually added to the silica-containing precursor under continuous stirring to obtain a homogeneous synthesis gel.

In the alkaline medium, silica is generally expected to react with sodium hydroxide to form soluble sodium silicate species because of the high solubility of silica under strongly basic conditions. Hydroxide ions promote the dissolution of silica, while sodium ions stabilize the resulting silicate species, providing

Accepted Manuscript - BCREC-20881 - 26 Nov 2026

the reactive building units required for zeolite crystallization. A simplified representation of this step, based on the literature and not verified experimentally in this study, is given as follows:

$$SiO_{2(aq)}+2NaOH_{(aq)}\rightarrow Na_2SiO_{3(aq)} + H_2O_{(aq)} \quad (4)$$

As commonly described in the literature, the high electronegativity of oxygen atoms in $SiO_2$ renders the silicon atoms more electropositive, facilitating nucleophilic attack by hydroxide ions to form the unstable intermediate $[SiO_2OH]^-$, which subsequently undergoes deprotonation. A second hydroxide ion reacts with the released proton to produce water, while two $Na^+$ ions balance the negative charge of the resulting silicate species ($SiO_3^{2-}$), leading to the formation of sodium silicate [8]. The subsequent addition of sodium aluminate to the sodium silicate solution resulted in the formation of a homogeneous aluminosilicate gel. This gel serves as the precursor for the hydrothermal crystallization of Beta zeolite. A simplified, non-stoichiometric representation of gel formation is given as follows:

$$NaAl(OH)_{4(aq)}+Na_2SiO_{3(aq)} \rightarrow [Na_x(AlO_2)_y(SiO_2)_2H_2O]_{(gel)} \quad (5)$$

The nucleation and crystal growth processes were initiated by the formation of an aluminosilicate gel during zeolite synthesis. During the hydrothermal treatment, the amorphous gel underwent structural rearrangement, leading to the formation of crystalline nuclei. As crystallization progressed, the amorphous gel gradually dissolved and served as the source of aluminosilicate species for crystal growth until a thermodynamically stable Beta zeolite framework formed, as generally described for zeolite crystallization [9].

### 3.2. Synthesis of NiW/Beta–γ-$Al_2O_3$ Catalyst

The preparation of the Beta–γ-$Al_2O_3$ support was carried out using the sol–gel method through several sequential steps. Initially, boehmite was mixed with the synthesized Beta zeolite, followed by the addition of deionized water. During this process, boehmite underwent hydration to form aluminum hydroxide, which acted as a precursor for the alumina binder. The reaction is represented as follows:

$$AlOOH_{(s)}+H_2O_{(aq)} \rightarrow AlOOH.H_2O_{(s)} \quad (6)$$

In the second step, nitric acid was added under continuous stirring to initiate the sol–gel process. The addition of nitric acid promoted the peptization of aluminum hydroxide, resulting in the formation of a homogeneous alumina sol. During this process, aluminum hydroxide reacted with nitric acid to produce aluminum nitrate and water, as represented by the following reaction:

$$AlOOH.H_2O_{(s)}+3HNO_{3(aq)}\rightarrow Al(NO_3)_{3(aq)} + 3H_2O_{(aq)} \quad (7)$$

After the formation of the alumina sol, ammonium hydroxide was added to induce gelation through the precipitation of aluminum hydroxide. The increase in pH promoted the hydrolysis of

Accepted Manuscript - BCREC 20881 - 26 Nov 2026

aluminum nitrate, resulting in the formation of aluminum hydroxide precipitates, as represented by the following reaction [10]

$$Al(NO_3)_{3(aq)} + 3NH_4OH_{(aq)} \rightarrow Al(OH)_{3(s)} + 3NH_4NO_{3(aq)} \quad (8)$$

The resulting aluminum hydroxide gel was extruded into a trilobe-shaped support and subsequently calcined at 550 °C for 5 h. Calcination was performed to promote the transformation of aluminum hydroxide into the γ-$Al_2O_3$ phase while improving the mechanical strength of the support. During this process, physically adsorbed water, residual organic species, and volatile impurities were removed, resulting in the formation of a thermally stable and porous support suitable for catalyst preparation.

The NiW/Beta–γ-$Al_2O_3$ catalyst was subsequently prepared by the incipient wetness impregnation method. The primary objective of the impregnation process was to achieve a uniform dispersion of the active Ni and W species throughout the pore network and surface of the Beta–γ-$Al_2O_3$ support, thereby producing a bifunctional catalyst. In this catalyst system, the NiW active phase provides hydrogenation–dehydrogenation functionality, whereas the Beta zeolite support supplies the acid sites required for hydrocarbon cracking. The synergistic interaction between the metallic and acidic functions is considered essential for enhancing catalytic activity and selectivity during the hydrocracking of Hydrotreated Vegetable Oil (HVO).

### 3.3. Catalyst Characterization

#### 3.3.1. XRD Patterns of the Catalysts

X-ray diffraction (XRD) analysis was performed to identify the crystalline phases of the synthesized Beta zeolite, catalyst supports, and NiW catalysts. The obtained diffraction patterns were compared with the standard reference from the International Centre for Diffraction Data (ICDD) database to confirm phase formation and crystallinity. Figure 1 presents the XRD patterns of Beta zeolite synthesized under hydrothermal crystallization temperatures of 135 and 170 °C, together with the reference diffraction pattern of Beta zeolite (ICDD No. 00-056-0467).

Accepted Manuscript - BCREC-20881 - 26 Nov 2025

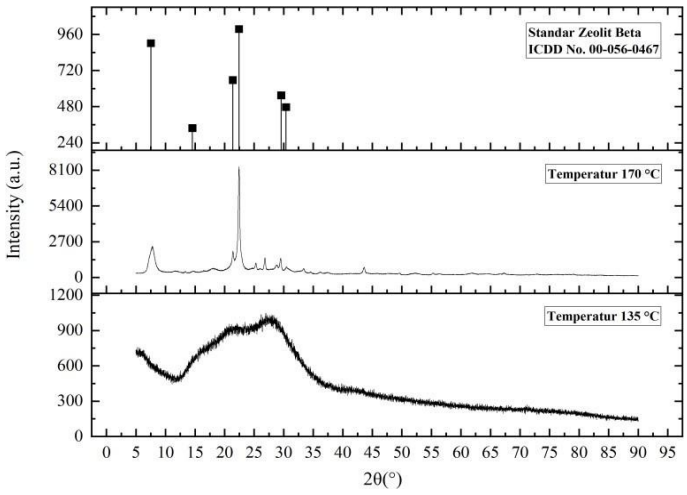



Figure 1 Diffraction Pattern of Synthesized Zeolite Beta

The XRD patterns revealed that the sample synthesized at a hydrothermal temperature of 135°C exhibited a predominantly amorphous structure, whereas the sample synthesized at 170°C showed well-defined crystalline diffraction peaks characteristic of Beta zeolite. Accordingly, the product obtained at 135°C was designated as amorphous Beta, while the sample synthesized at 170°C was identified as crystalline Beta zeolite. These results indicate that the hydrothermal crystallization temperature plays a crucial role in the formation of the zeolite framework. Increasing the hydrothermal temperature promotes nucleation and crystal growth, resulting in higher crystallinity, consistent with the findings reported by [11]

The sample synthesized at 135°C exhibited major diffraction peaks at 2θ = 5.37° and 27.56°, indicating the absence of a well-developed Beta zeolite framework. In contrast, the sample synthesized at 170 °C showed characteristic diffraction peaks at 2θ = 7.77°, 21.40°, and 22.43°. These peaks closely correspond to the standard diffraction pattern of Beta zeolite (ICDD No. 00-056-0467), which displays characteristic reflections at 2θ = 7.53°, 11.61°, 21.39°, 22.43°, and 25.33°. The close agreement between the synthesized sample and the reference pattern confirms the successful formation of crystalline Beta zeolite at a hydrothermal temperature of 170°C.

To further evaluate the crystalline phases after catalyst preparation, XRD analysis was performed on the synthesized catalysts and the reference catalyst. The diffraction patterns of the synthesized catalysts and the reference catalyst are presented in Figure 2.

Accepted Manuscript - BCREC 20881 - 26 Nov 2026

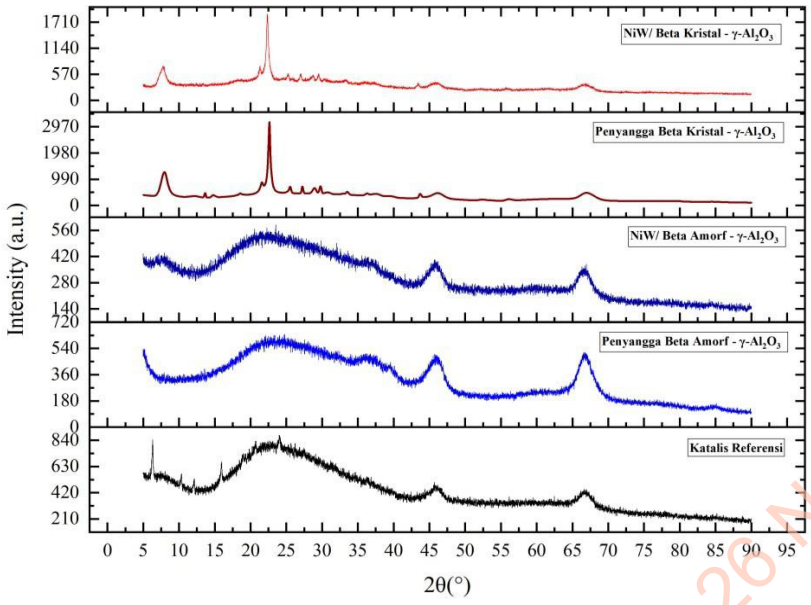



Figure 2 Diffraction Patterns of the Synthesized Catalyst and the Reference Catalyst

Figure 2 shows that both synthesized catalysts exhibit the same crystalline phases as their respective supports. Based on the diffraction patterns and peak intensities, the catalysts can be ranked in descending order of crystallinity as NiW/Crystalline Beta–γ-$Al_2O_3$, the reference catalyst, and NiW/Amorphous Beta–γ-$Al_2O_3$. This result indicates that the NiW/Crystalline Beta–γ-$Al_2O_3$ catalyst possesses higher crystallinity than the reference catalyst.

3.3.2. XRF Analysis

The XRF analysis results presented in Table 1 show that the NiW/Amorphous Beta–γ-$Al_2O_3$ catalyst contains higher Ni and W contents than the NiW/Crystalline Beta–γ-$Al_2O_3$ catalyst.

Table 1. Active metal concentration of the catalysts

| Sample | NiO [wt.%] | $WO_3$ [wt.%] |
|---|---|---|
| NiW/Amorphous Beta–γ-$Al_2O_3$ | 2.54 | 17.50 |
| NiW/Crystalline Beta–γ-$Al_2O_3$ | 2.00 | 15.60 |
| Reference Catalyst | 1.80 | 13.00 |

The XRF results in Table 1 show that the active metals Ni and W were successfully impregnated onto all of the synthesized catalysts. The NiW/Amorphous Beta–γ-$Al_2O_3$ catalyst had the highest NiO and $WO_3$ contents, at 2.54 wt.% and 17.50 wt.%, respectively, followed by NiW/Crystalline Beta–γ-$Al_2O_3$ at 2.00 wt.% and 15.60 wt.%, whereas the reference catalyst contained 1.80 wt.% NiO and 13.00 wt.% $WO_3$. These results show that both synthesized catalysts had higher active metal contents than the reference

Accepted Manuscript - BCREC-20881 - 26 Nov 2026

catalyst. This difference may be related to the characteristics of the supports, particularly their specific surface area, pore volume, and pore diameter, as well as the interaction between the metal precursors and the support surface during impregnation. These characteristics influence the amount of metal that can be deposited and its distribution on the catalyst surface.

When related to the crystal structure and textural characterization results, the difference in active metal content should also be considered in terms of the characteristics of each support. The crystalline structure of Beta zeolite has an ordered pore system and aluminosilicate framework, which may give rise to active-site environments with particular characteristics. In contrast, the amorphous Beta support has a less ordered structure, so its metal deposition behavior may differ. However, the amount of impregnated metal is determined not only by the crystal structure but also by the surface area and pore accessibility of the support.

Notably, the NiW/Crystalline Beta–γ-$Al_2O_3$ catalyst, whose Ni and W contents were lower than those of NiW/Amorphous Beta–γ-$Al_2O_3$ but higher than those of the reference catalyst, was selected for performance testing. This suggests that catalytic activity is determined not only by the total amount of active metal, but also by metal dispersion, metal–support interaction, and the acidity of the catalyst. In hydrocracking, Ni contributes the hydrogenation and dehydrogenation function, whereas W, together with Ni, contributes to the formation of the active NiWS phase after sulfiding. The acid sites of the support, in turn, are involved in protonation, C–C bond cleavage, and the formation of hydrocarbon products with lower boiling ranges.

Accordingly, the lower active metal content of NiW/Crystalline Beta–γ-$Al_2O_3$ does not necessarily imply limited catalytic activity. The combination of crystal structure, textural properties, metal distribution, and acidity may produce a more effective synergy between the metal and acid functions in hydrocracking. These results also suggest that optimizing the support characteristics and the distribution of the active metal is an important aspect of developing hydrocracking catalysts. However, because the metal loadings of the catalysts differ, the contribution of each factor cannot be separated based on the present data. Based on these characterization results, the NiW/Crystalline Beta–γ-$Al_2O_3$ catalyst was selected as the optimal catalyst for performance testing, and its metal content was higher than that of the reference catalyst [12].

3.3.3. Surface Area Analysis

The Surface Area Analyzer (SAA) was employed to determine the specific surface area, pore diameter, and pore volume of the synthesized catalysts. The textural properties obtained from the Surface Area Analyzer are summarized in Table 2.

Accepted Manuscript - BCREC-20884 - 26 Nov 2026

Table 2. Textural properties of the zeolites, supports, and catalysts determined by SAA

| Sample | Surface Area [$m^2\ g^{-1}$] | Pore Volume [$cm^3\ g^{-1}$] | Pore Diameter [Å] |
|---|---|---|---|
| Amorphous Beta | 240.89 | 0.29 | 49 |
| Amorphous Beta Support | 285.54 | 0.57 | 79 |
| NiW/Amorphous Beta–γ-$Al_2O_3$ | 250.39 | 0.41 | 60 |
| Crystalline Beta | 317.03 | 0.21 | 27 |
| Crystalline Beta Support | 342.49 | 0.52 | 61 |
| NiW/Crystalline Beta–γ-$Al_2O_3$ | 331.36 | 0.43 | 52 |
| Reference Catalyst | 267.51 | 0.46 | 68 |

Based on the data presented in Table 2, the specific surface area, pore volume, and pore diameter of the catalyst supports were higher than those of the parent zeolites. This increase can be attributed to the incorporation of γ-$Al_2O_3$ as a binder during support preparation. The γ-$Al_2O_3$ binder is known to possess high porosity, a large specific surface area, and a uniform pore structure [5]. Among the impregnated catalysts, the NiW/Crystalline Beta–γ-$Al_2O_3$ catalyst showed a higher specific surface area (331.36 $m^2\ g^{-1}$) and a comparable pore volume (0.43 $cm^3\ g^{-1}$) relative to the NiW/Amorphous Beta–γ-$Al_2O_3$ catalyst (250.39 $m^2\ g^{-1}$ and 0.41 $cm^3\ g^{-1}$), whereas its pore diameter was smaller (52 versus 60 Å).

The specific surface area of the catalysts decreased after metal impregnation compared with that of the corresponding supports. A high specific surface area is beneficial for catalytic activity because it provides more exposed active sites for the dispersion of the active phase [13]. The reduction in surface area after impregnation is attributed to the deposition of NiW species on the support surface and within its pore structure. As the amount of deposited metal increases, the accessible surface area decreases because the active metal species partially cover the support surface and block a portion of the pores [14]

3.3.4. Surface Acidity Analysis by $NH_3$-TPD

The surface acidity of the synthesized catalysts was evaluated using temperature-programmed desorption of ammonia ($NH_3$-TPD) to determine the total amount of acid sites. The acidity was characterized based on the adsorption–desorption of ammonia, where the amount of adsorbed $NH_3$ reflects the total number of acidic sites in the zeolite. A higher amount of desorbed $NH_3$ indicates a greater total acidity of the catalyst [15]. The $NH_3$-TPD results are summarized in Table 3.

Accepted Manuscript - BCREC-20881 - 26 Nov 2026

Table 3. Total acidity of the zeolites, supports, and catalysts determined by $NH_3$-TPD

| Sample | Acidity (mmol $g^{-1}$) |
|---|---|
| | Total |
| Amorphous Beta | 0.41 |
| Amorphous Beta Support | 0.65 |
| NiW/Amorphous Beta–γ-$Al_2O_3$ | 1.47 |
| Crystalline Beta | 3.31 |
| Crystalline Beta Support | 1.64 |
| NiW/Crystalline Beta–γ-$Al_2O_3$ | 1.66 |
| Reference Catalyst | 0.54 |

Based on the $NH_3$-TPD results presented in Table 3, crystalline Beta zeolite exhibited the highest total acidity of 3.31 mmol $g^{-1}$, which was substantially higher than that of amorphous Beta (0.41 mmol $g^{-1}$). This result indicates that the formation of the crystalline Beta zeolite framework contributes to an increase in the number of acidic sites, suggesting that crystallinity is one of the key factors governing the acidic properties of the material. After the preparation of the catalyst support, the total acidity decreased to 1.64 mmol $g^{-1}$ for the Crystalline Beta–γ-$Al_2O_3$ support and 0.65 mmol $g^{-1}$ for the Amorphous Beta–γ-$Al_2O_3$ support. This decrease may be attributed to the incorporation of γ-$Al_2O_3$ as a binder, which is known to reduce the density of acidic sites through dilution of the zeolite phase, as reported by [16].

Following the impregnation of the active Ni and W metals, the total acidity increased to 1.66 mmol $g^{-1}$ for the NiW/Crystalline Beta–γ-$Al_2O_3$ catalyst and 1.47 mmol $g^{-1}$ for the NiW/Amorphous Beta–γ-$Al_2O_3$ catalyst. The increase was marginal for the crystalline sample (1.64 mmol $g^{-1}$ for its support) but more pronounced for the amorphous sample (0.65 mmol $g^{-1}$ for its support), which suggests that the introduced Ni and W species may provide additional $NH_3$ adsorption sites. The NiW/Crystalline Beta–γ-$Al_2O_3$ catalyst therefore showed a higher total acidity than both the NiW/Amorphous Beta–γ-$Al_2O_3$ catalyst and the reference catalyst (0.54 mmol $g^{-1}$). According to [17], amorphous silica–alumina materials generally exhibit lower acidity than crystalline zeolites. Furthermore [2] reported that the acid sites of the zeolite component play a crucial role in hydrocracking reactions by serving as the active centers for carbocation formation, which initiates C–C bond cleavage. Therefore, the higher total acidity of the NiW/Crystalline Beta–γ-$Al_2O_3$ catalyst is expected to be favorable for its hydrocracking performance.

3.4. Catalytic Performance Evaluation

Accepted Manuscript - BCREC-20881 - 26 Nov 2026

Catalytic performance testing was carried out only on the synthesized NiW/Crystalline Beta–γ-$Al_2O_3$ catalyst, and the reference catalyst was tested under the same conditions for comparison. This choice was based on the characterization results, which consistently identified the crystalline Beta catalyst as the most suitable candidate for hydrocracking. First, XRD showed that the zeolite synthesized at 135 °C was predominantly amorphous, whereas the one synthesized at 170 °C had the well-defined Beta framework (Section 3.3.1). Second, the NiW/Crystalline Beta–γ-$Al_2O_3$ catalyst had a higher specific surface area than the NiW/Amorphous Beta–γ-$Al_2O_3$ catalyst (331.36 versus 250.39 $m^2\ g^{-1}$) and a higher total acidity (1.66 versus 1.47 mmol $g^{-1}$), and its total acidity was about three times that of the reference catalyst (0.54 mmol $g^{-1}$) (Sections 3.3.3 and 3.3.4). Third, its metal content (2.00 wt.% NiO and 15.60 wt.% $WO_3$) was close to the target loadings (2 and 15 wt.%) and higher than that of the reference catalyst (Section 3.3.2). Since hydrocracking requires the cracking function of the acid sites to work together with the hydrogenation function of the NiW phase, a catalyst based on a poorly crystallized support with lower surface area and acidity was not considered a competitive candidate. Testing was therefore focused on the catalyst that the characterization pointed to, and the reference catalyst served as the benchmark. The amorphous catalyst was characterized but not tested, and the consequences of this are discussed in Section 3.4.

The catalytic performance of the NiW/Crystalline Beta–γ-$Al_2O_3$ catalyst (hereafter, the synthesized catalyst) and the reference catalyst was evaluated to investigate their hydrocracking activity toward Hydrotreated Vegetable Oil (HVO) as a model feedstock. Prior to the catalytic reaction, all catalysts were activated through a sulfidation process. Sulfidation was performed to convert the catalyst from the inactive oxide phase into the catalytically active sulfide phase. According to the literature, tungsten species after calcination are present mainly as crystalline $WO_3$, $WO_4$, or $Al_2(WO_4)_3$, which are subsequently transformed into the active $WS_2$ phase during sulfidation. This activation process is reported to generate catalytically active species, including NiWS, NiS, $Ni^{2+}$, $WS_2$, $WS_xO_y$, and $W^{6+}$, which are responsible for the hydrogenation–dehydrogenation function of hydrocracking catalysts [18]. The sulfided phase of the catalysts in this study was not characterized (see the limitations below).

The liquid products obtained from the hydrocracking of Hydrotreated Vegetable Oil (HVO) were analyzed using GC-SIMDIS to determine the distribution of hydrocarbon fractions, with particular emphasis on the naphtha ($C_6$–$C_{10}$) and kerosene ($C_{11}$–$C_{14}$) fractions. The conversion calculated from the GC-SIMDIS data using Equation (1) is presented in Figure 3.

Accepted Manuscript - BCREC-20881 - 26 Nov 2026

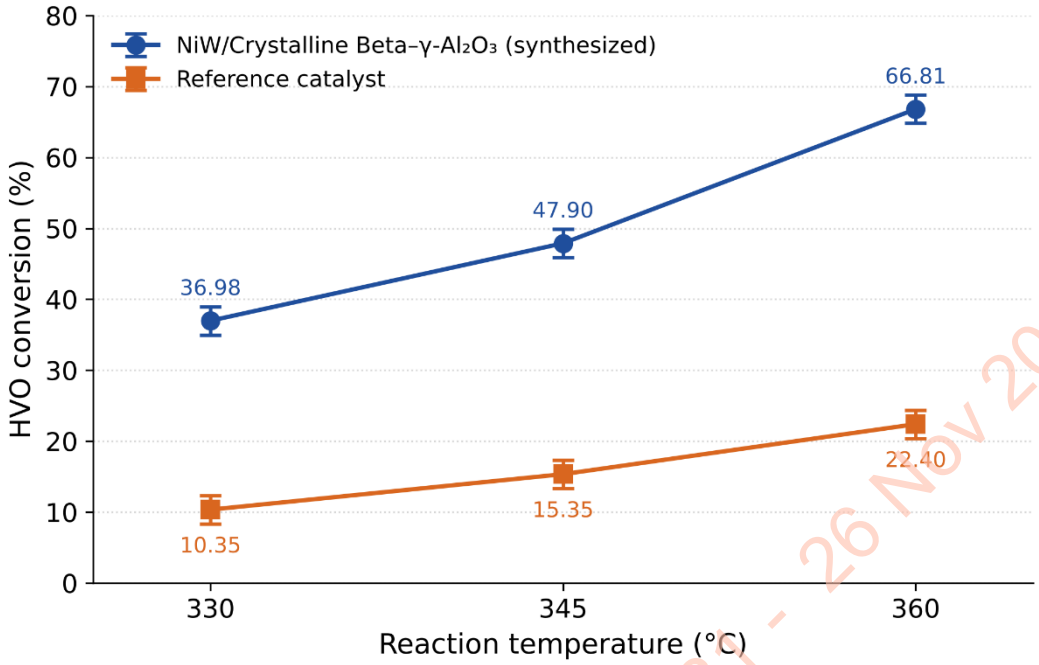



Figure 3 HVO Hydrocracking Conversion

As shown in Figure 3, the synthesized catalyst exhibited the highest conversion of 66.81% at a reaction temperature of 360 °C, whereas the reference catalyst achieved a maximum conversion of 22.40% under the same reaction conditions. It can also be observed that the conversion of both the NiW/Crystalline Beta–γ-$Al_2O_3$ catalyst and the reference catalyst increased with increasing reaction temperature. This trend is consistent with the acceleration of cracking reactions at higher temperature. The conversions obtained over the synthesized catalyst at 330, 345, and 360°C were 36.98%, 47.90%, and 66.81%, respectively, while those of the reference catalyst were 10.35%, 15.35%, and 22.40%, respectively. The higher conversion achieved by the synthesized catalyst indicates its higher catalytic activity for the hydrocracking of HVO under the tested conditions, although the difference in metal loading (Table 1) should also be considered.

The synthesized catalyst exhibited higher conversion than the reference catalyst, which can be associated with its higher active metal loading and total acidity. The synthesized catalyst contained 2.00 wt.% NiO and 15.60 wt.% $WO_3$, whereas the reference catalyst contained 1.80 wt.% NiO and 13.00 wt.% $WO_3$ (Table 1). In addition, the synthesized catalyst possessed a total acidity of 1.66 mmol $g^{-1}$, which was approximately three times that of the reference catalyst (0.54 mmol $g^{-1}$; Table 3). According to [6] differences in acidity are among the main factors governing variations in catalytic activity and product selectivity. The higher conversion achieved by the synthesized catalyst is therefore attributed mainly to its Beta zeolite component, which provides a higher total acidity and thereby promotes the cracking reactions more effectively than the reference catalyst. Because the metal loading and the zeolite content of the two catalysts differ, the contribution of each factor cannot be separated based on the present data.

Accepted Manuscript - BCREC-20881 - 26 Nov 2026

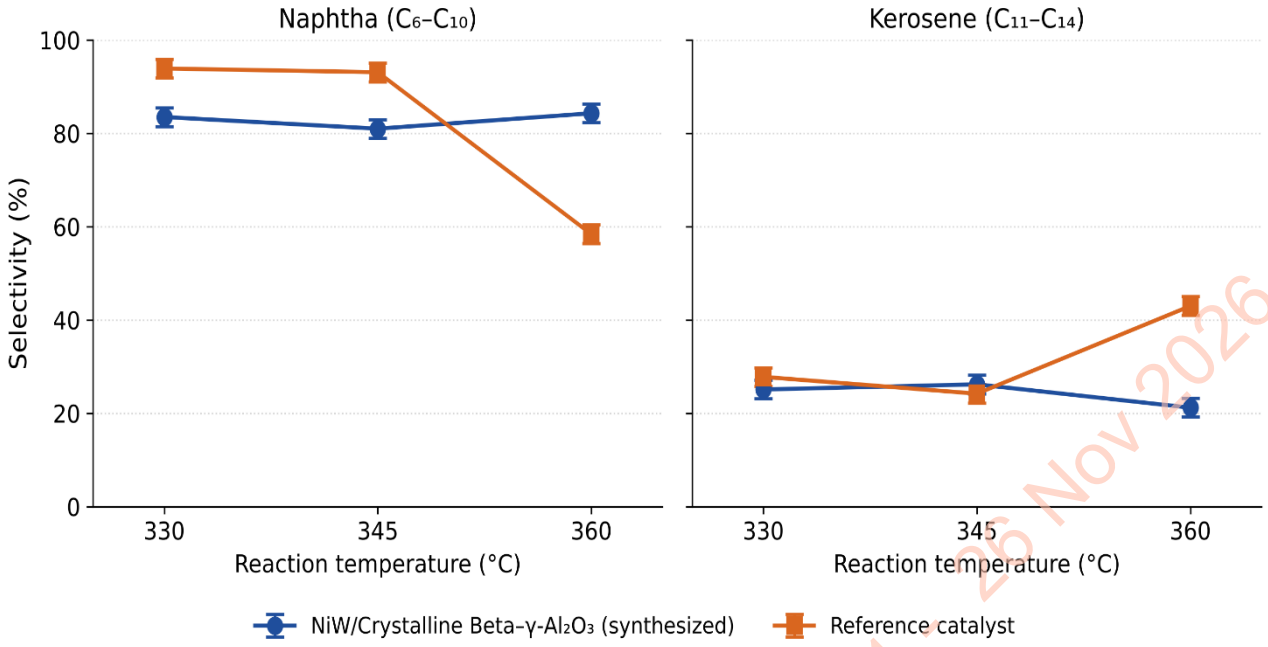



Figure 4 Selectivity of NiW/Beta - γ-Al2O3 Catalyst and Catalyst

As shown in Figure 4, each catalyst exhibited a different product selectivity. Selectivity refers to the ability of a catalyst to promote the desired reaction while minimizing the formation of undesired by-products. Both the synthesized catalyst and the reference catalyst exhibited high selectivity toward the naphtha fraction, which may be related to their acidic properties. The differences in product selectivity among the catalysts may be attributed to the zeolite structure and the availability of acidic sites within each catalyst, as reported by [19]

Table 4. Total concentration of gaseous by-products ($C_1$–$C_6$) in the hydrocracking products

| Catalyst | Temperature [°C] | Component | Total Concentration [%] |
|---|---|---|---|
| NiW/Crystalline Beta–γ-$Al_2O_3$ | 330 | $C_1$–$C_6$ | 14.05 |
| | 345 | $C_1$–$C_6$ | 17.82 |
| | 360 | $C_1$–$C_6$ | 17.94 |
| Reference | 330 | $C_1$–$C_6$ | 1.68 |
| | 345 | $C_1$–$C_6$ | 2.43 |
| | 360 | $C_1$–$C_6$ | 2.98 |

As presented in Table 4 both catalysts produced gaseous by-products with carbon distributions ranging from $C_1$ to $C_6$. The total concentrations of gaseous by-products generated by the synthesized

Accepted Manuscript - BOREC-20881 - 26 Nov 2026

catalyst at reaction temperatures of 330, 345, and 360 °C were 14.05%, 17.82%, and 17.94%, respectively, whereas those produced by the reference catalyst were 1.68%, 2.43%, and 2.98%, respectively. The formation of these gaseous products suggests that secondary cracking (overcracking) may have occurred during the hydrocracking process, which may be associated with the relatively high acidity of the catalyst. Because the gas flow rate was not recorded, only the relative composition of the gas is reported, and the gaseous yield and the extent of overcracking could not be quantified. [20] reported that a high density of acid sites promotes secondary cracking reactions, leading to decreased product selectivity and increased formation of light gaseous hydrocarbons.

Several limitations of this study should be noted. The catalytic tests were performed only on the crystalline catalyst, whose metal loading differs from that of the reference catalyst; therefore, the effect of the crystallization temperature cannot be separated from that of the metal loading. The acidity was evaluated only as the total amount of $NH_3$ desorbed, so the nature of the acid sites was not assessed. The sulfided phase and sulfur retention during HVO conversion were not characterized. Independent replicate runs, uncertainty estimates, carbon balances, catalyst durability, and heat- and mass-transfer limitations were not evaluated. Accordingly, the reported trends are indicative, and these aspects should be addressed in future work.

## 4. Conclusions

Beta zeolite was successfully synthesized via the hydrothermal method at a crystallization temperature of 170 °C, as confirmed by X-ray diffraction (XRD) analysis. The use of crystalline Beta zeolite as a catalyst support resulted in a NiW/Crystalline Beta–γ-$Al_2O_3$ catalyst with more favorable physicochemical properties than the NiW/Amorphous Beta–γ-$Al_2O_3$ catalyst, as evidenced by its higher specific surface area and total acidity, which are expected to provide a greater number of catalytically active sites. In addition, increasing the reaction temperature enhanced the hydrocracking conversion for both catalysts. The NiW/Crystalline Beta–γ-$Al_2O_3$ catalyst was tested in the hydrocracking of HVO and achieved a maximum conversion of 66.81% at 360 °C, which was higher than that of the reference catalyst (22.40%) under the same operating conditions. These findings suggest that the crystalline framework of Beta zeolite contributes to improved physicochemical properties and hydrocracking performance, together with the hydrogenation function of the NiW active phase. Because the amorphous catalyst was not tested and the metal loadings differ, the effect of the crystallization temperature cannot be separated from that of the metal loading.

Accepted Manuscript - BCREC-20821 - 26 Nov 2026

**Acknowledgements**

The authors gratefully acknowledge PT Pertamina (Persero) for providing the facilities and support required to conduct this research. The authors also express their sincere appreciation to Syifa Urrohmah for her assistance with catalyst performance testing at the Materials and Catalysts Laboratory.

## References


[1] Valavarasu, G., Sairam, B. (2013). Hydrocracking of Vacuum Gas Oil: Conversion, Product Yields, and Product Quality over an Industrial Hydrocracking Catalyst System. *Petroleum Science and Technology*, 31(6), 551–562. DOI: 10.1080/10916466.2010.516296.

[2] Dik, P.P., Danilova, I.G., Golubev, I.S., Kazakov, M.O., Nadeina, K.A., Budukva, S. V., Pereyma, V.Y., Klimov, O. V., Prosvirin, I.P., Gerasimov, E.Y., Bok, T.O., Dobryakova, I. V., Knyazeva, E.E., Ivanova, I.I., Noskov, A.S. (2019). Hydrocracking of Vacuum Gas Oil over NiMo/zeolite-Al2O3: Influence of Zeolite Properties. *Fuel*, 237, 178–190. DOI: 10.1016/j.fuel.2018.10.012.

[3] Anggoro, D.D. (2017). *Buku Ajar Teori dan Aplikasi Rekayasa Zeolit*. Undip Press.

[4] Ikuno, T., Chaikittisilp, W., Liu, Z., Iida, T., Yanaba, Y., Yoshikawa, T., Kohara, S., Wakihara, T., Okubo, T. (2015). Structure-Directing Behaviors of Tetraethylammonium Cations toward Zeolite Beta Revealed by the Evolution of Aluminosilicate Species Formed during the Crystallization Process. *Journal of the American Chemical Society*, 137(45), 14533–14544. DOI: 10.1021/jacs.5b11046.

[5] Almulla, F.M., Ali, S.A., Aldossary, M.R., Alnaimi, E.I., Zholobenko, V.I., Jumah, A. bin, Garforth, A.A. (2021). On the influence of alumina as a binder on the performance of Pt-Beta catalyst during the transalkylation of toluene and 1,2,4-Trimethylbenzene. *Microporous and Mesoporous Materials*, 320 DOI: 10.1016/j.micromeso.2021.111095.

[6] Bukhtiyarova, M. V., Toktarev, A. V., Kazakov, M.O., Kodenev, E.G., Pereyma, V.Y., Gabrienko, A.A., Bukhtiyarov, A. V., Echevsky, G. V. (2020). Effect of Sulfosalicylic Acid Treatment on the Properties of Beta Zeolite and Performance of NiW/Beta-based Catalysts in Hexadecane Hydrocracking. *Applied Catalysis A: General*, 598 DOI: 10.1016/j.apcata.2020.117573.

[7] Manrique, C., Guzman, A., Perez-Pariente, J., Marquez-Alvarez, C., Echavarria, A. (2016). Effect of Synthesis Conditions on Zeolite Beta Properties and its Performance in Vacuum Gas Oil Hydrocracking Activity. *Microporous and Mesoporous Materials*, 347–360. DOI: 10.1016/j.micromeso.2016.07.017.

[8] Dwi Rasy Mujiyanti, Nuryono Nuryono, Eko Kunarti (2010). *Sintesis dan Karakterisasi Silika Gel dari Abu Sekam Padi yang Dimoblisasi dengan 3-(Trimetoksisilil)-1-Propantiol*.

[9] Dan Karakterisasi Zeolit Berbahan Dasar, S., Hawa Syaifie, P., Ayu Paramita Kusumah Wardhani, G., Agus Taufiq, dan, Studi Kimia, P., Nusa Bangsa Jl Sholeh Iskandar Km, U.K., Sareal, T., Barat, J., Studi PMIP, P., AKA Bogor Jl Pangeran Sogiri No, P., Baru, T., Utara, B. (2019). Synthesis and Characterization of Zeolite from Karawang Rice Husk Ash

[10] Zhang, B. (2021). Hydroprocessing and the Chemistry. Hydroprocessing Catalysts and Processes: The Challenges For Biofuels Production

[11] Deni Fajar Fitriyana, Sulardjaka Sulardjaka, Norman Iskandar, Muhammad Zulfikar (2018). Pengaruh Konsentrasi NaOH Terhadap Ukuran Kristal Zeolit A Yang Disintesis Dari Limbah

[12] Cui, G., Wang, J., Fan, H., Sun, X., Jiang, Y., Wang, S., Liu, D., Gui, J. (2011). Towards understanding the microstructures and hydrocracking performance of sulfided Ni-W catalysts: Effect of metal loading. *Fuel Processing Technology*, 92(12), 2320–2327. DOI: 10.1016/j.fuproc.2011.07.020.

[13] Bolton, S., Bon, C. (2010). *Pharmaceutical statistics : Practical and Clinical Applications*, 5th ed. New York: Informa Healthcare USA.


Accepted Manuscript - BCREC 20881 - 26 Nov 2026

[14] Wang, Y., Gan, Y., Whiting, R., Lu, G. (2009). Synthesis of Sulfated Titania Supported on Mesoporous Silica Using Direct Impregnation and its Application in Esterification of Acetic Acid and n-Butanol. *Journal of Solid State Chemistry*, 182(9), 2530–2534.

[15] Robinson, P.R., Dolbear, G.E. (2007). Hydrotreating and Hydrocracking: Fundamentals. In: *Practical Advances in Petroleum Processing*. Springer New York, pp. 177–218.DOI: 10.1007/978-0-387-25789-1_7.

[16] Sano, Y., Sugahara, K., Choi, K.H., Korai, Y., Mochida, I. (2005). Two-step Adsorption Process for Deep Desulfurization of Diesel Oil. *Fuel*, 84, 903–910.

[17] Kazakov, M.O., Nadeina, K.A., Danilova, I.G., Dik, P.P., Klimov, O. V., Pereyma, V.Y., Paukshtis, E.A., Golubev, I.S., Prosvirin, I.P., Gerasimov, E.Y., Dobryakova, I. V., Knyazeva, E.E., Ivanova, I.I., Noskov, A.S. (2019). Influence of USY zeolite recrystallization on physicochemical properties and catalytic performance of NiMo/USY-Al 2 O 3 hydrocracking catalysts. *Catalysis Today*, 329, 108–115. DOI: 10.1016/j.cattod.2019.01.003.

[18] Minaev, P.P., Nikulshina, M.S., Gulyaeva, L.A., Ovsienko, O.L., Khavkin, V.A., Shmel'kova, O.I., Nikulshin, P.A. (2017). Hydrotreating of Vacuum Gas Oil on NiW/Al2O3 Catalysts Prepared with the Use of Chelating Agents. *Petroleum Chemistry*, 57(12), 1161–1164. DOI: 10.1134/S0965544117060214.

[19] Kazakov, M.O., Nadeina, K.A., Danilova, I.G., Dik, P.P., Klimov, O. V., Pereyma, V.Y., Gerasimov, E.Y., Dobryakova, I. V., Knyazeva, E.E., Ivanova, I.I., Noskov, A.S. (2018). Hydrocracking of vacuum gas oil over NiMo/Y-Al2O3: Effect of mesoporosity introduced by zeolite Y recrystallization. *Catalysis Today*, 305, 117–125. DOI: 10.1016/j.cattod.2017.08.048.

[20] Golubev, I.S., Dik, P.P., Kazakov, M.O., Pereyma, V.Y., Klimov, O. V., Smirnova, M.Y., Prosvirin, I.P., Gerasimov, E.Y., Kondrashev, D.O., Golovachev, V.A., Vedernikov, O.S., Kleimenov, A. V., Noskov, A.S. (2021). The Effect of Si/Al Ratio of Zeolite Y in NiW Catalyst for Second Stage Hydrocracking. *Catalysis Today*, 378, 65–74. DOI: 10.1016/j.cattod.2021.01.014.

Accepted Manuscript - BCREC-20981 - 06 Nov 2026